



Analysis of laminar forced convection with Network Simulation in thermal entrance region of ducts

J. Zueco ^a, F. Alhama ^b, C.F. González Fernández ^{b,*}

^a *Department of Thermic Engineering and Fluids, University Politechnique of Cartagena, Campus Muralla del Mar, 30203 Cartagena, Spain*

^b *Department of Applied Physics, University Politechnique of Cartagena, Campus Muralla del Mar, 30203 Cartagena, Spain*

Received 5 December 2001; accepted 9 October 2003

Abstract

The transient heat transfer problem referring to a fully laminar flow developing in pipes exposed to a step change in the temperature is studied here. Bi-dimensional (axial–radial) wall and fluid heat conduction are assumed. The effects of pipe thickness, Péclet number, wall-to-fluid conductivity ratio and thermal diffusivity ratio are determined in the solutions. Boundary condition other than isothermal may easily be incorporated in the model with no special requirements. The numerical procedure employed permits the solution for both transient and steady-state problems at the same time, and its programming does not require manipulation of the sophisticated mathematical software that is inherent in other numerical methods. The network simulation method, which satisfies the conservation law for the heat flux variable and the uniqueness law for temperature, also permits the direct visualisation and evolution of the local and/or integrated transport variables at any point or section of the medium.

© 2003 Elsevier SAS. All rights reserved.

Keywords: Transient heat conduction; Conjugate problem; Network simulation method

1. Introduction

In recent years, numerous authors have published papers on the stationary conjugate (conduction–convection) heat transfer problem in laminar flow in pipes under different sets of boundary conditions, a kind of problem first proposed by Graetz [1,2]. Mori et al. [3] investigated the effects of wall conduction, both for parallel plates and circular pipes, under the known boundary conditions of the first and second kind; Michelsen and Willadsen [4], Pagliarini [5], Vick and Özisik [6] studied Graetz's problem with axial conduction in the pipe and fluid, and determined the range of Péclet numbers for which axial conduction is negligible. For the same problem, Wijesundera [7] and Guedes et al. [8] obtained solutions for a convective boundary condition. The effect of internal heat generation was studied by Zhang et al. [9], while Zariffteh et al. [10] and Campo and Rangel [11] studied the conjugate effect of 1-D wall and

fluid axial conduction. More recently Bilir [12,13] included the effect of 2-D (radial–axial) wall and fluid conduction for low Péclet numbers in large circular pipes whose external constant temperature changes sharply at a given section. For transient problems Cotta et al. [14] and Weigong and Kakac [15] obtained solutions for a periodic variation of the input temperature in ducts of constant thickness, which had previously been studied by Olek et al. [16] and Wei-Mon [17], the latter including a convective boundary condition.

In this paper, we study the heat transfer transient-state related to a fully development laminar flow in circular pipes. Bi-dimensional (axial–radial) wall and fluid heat conduction is considered and the effects of Péclet number and the pipe thickness are analysed. Internal heat generation in the fluid due to dissipation terms, thermal properties dependent of the temperature, convective boundary conditions and other kinds of initial and/or boundary conditions are easily implemented with no special requirements in the model.

The numerical tool employed to solve this problem is the Network Simulation Method (NSM). This general purpose technique, briefly described in the appendix, has

* Corresponding author.

E-mail address: carlosf.gonzalez@upct.es (C.F. González Fernández).

Nomenclature

A	ratio of diffusivities, α_s/α_f
c_e	specific heat
C	capacitor
C	constant
k	thermal conductivity
G	control-voltage current-source
L	thickness of the pipe
l	L/R ratio
N	number of cells
Nu	Nusselt number
Pe	Péclet number
q	heat flux
r	radial co-ordinate
R	inner radius of the pipe
R	resistor
t	time
T	temperature
T_I, T_{II}	constant temperature
z	axial co-ordinate

Δr	radial thickness of the cell
Δz	axial thickness of the cell
α	diffusivity
ρ	density

Subscripts

b	bulk
co	axial convection
f	associated to fluid
i, j	associated with i, j nodal point
$i, i - \Delta, i + \Delta$	associated to the centre, left and right position on the cell
m	medium value
o	dimensionless quantity
r	radial
s	associated to solid
tran	transitory regime
w	solid–fluid interface
z	axial

been applied successfully to a great variety of lineal and non-lineal transport problems [18–20]. NSM takes the partial differential equations that define the mathematical model of the physical process, and by means of spatial discretization, yields the ordinary differential equations which are the basis for implementing the standard electrical network model for an elemental control volume. The main advantage (even for complicated non-lineal problems) is that the network model is comprised by very few electrical devices connected in series to which the boundary conditions are added to form the whole model of the medium. The network for the problem here studied is included in the mentioned appendix. The simulation is carried out in a PC using suitable software, PSPICE® in this work [21].

2. Physical and mathematical model

Fig. 1 shows the system studied: a long pipe, whose outer surface temperature has a jump discontinuity at a given section. The fluid flow is considered to be hydro-

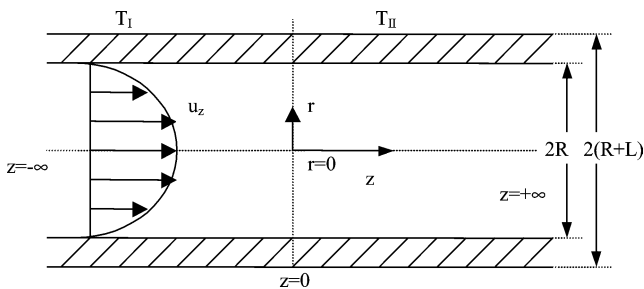


Fig. 1. Geometry of the problem.

dynamically developed, with no viscous dissipation, and the thermal properties of the fluid and pipe are constant (other kinds of boundary condition, including heat generation due to viscous dissipation, may easily be assumed by the numerical method used).

Under these conditions, the set of governing equations or mathematical model can be formulated as follows:

$$(1/r)(\partial[(rk_s)\partial T_s/\partial r]/\partial r) + (\partial[k_s\partial T_s/\partial z]/\partial z) = (\rho c_e)_s \partial T_s/\partial t \quad (1a)$$

$$(1/r)(\partial[(rk_f)\partial T_f/\partial r]/\partial r) + (\partial[k_f\partial T_f/\partial z]/\partial z) = (\rho u_z c_e)_f \partial T_f/\partial z + (\rho c_e)_f \partial T_f/\partial t \quad (1b)$$

Eqs. (1a) and (1b) refer to the solid and liquid regions, respectively. For the Graetz problem, which is used for comparison, only Eq. (1b) is needed, the transitory term being omitted. In order to generalise the solution, the above equations and the initial and boundary conditions may be written in dimensionless form, resulting in

$$(1/r_o)(\partial[r_o\partial T_{o,s}/\partial r_o]/\partial r_o) + (1/Pe^2)(\partial[\partial T_{o,s}/\partial z_o]/\partial z_o) = 1/A(\partial T_{o,s}/\partial t_o) \quad (2a)$$

$$(1/r_o)(\partial[r_o\partial T_{o,f}/\partial r_o]/\partial r_o) + (1/Pe^2)(\partial[\partial T_{o,f}/\partial z_o]/\partial z_o) = (1 - r_o^2)(\partial T_{o,f}/\partial z_o) + (\partial T_{o,f}/\partial t_o) \quad (2b)$$

and Eqs. (3a)–(3j), (4) in Table 1, where

$$T_o = (T - T_I)/(T_{II} - T_I)$$

$$z_o = z/(RPe), \quad r_o = r/R, \quad l_o = L/R$$

$$t_o = t\alpha_f/R^2, \quad u_z = 2u_m[1 - (r/R)^2]$$

$$Pe = (2u_m R)/\alpha_f, \quad k_{sf} = k_s/k_f, \quad A = \alpha_s/\alpha_f$$

α being the diffusivity, $\alpha = k(\rho c_e)^{-1}$. For most practical applications, the interfacial heat flux, bulk temperature and local Nusselt number are required. These values may be computed from

$$q_{w,o} = \left(\frac{\partial T_{o,f}}{\partial r_o} \right)_{r_o=1} \quad (5a)$$

$$T_{b,o} = 4 \int_0^1 r_o (1 - r_o^2) T_{o,f} dr_o \quad (5b)$$

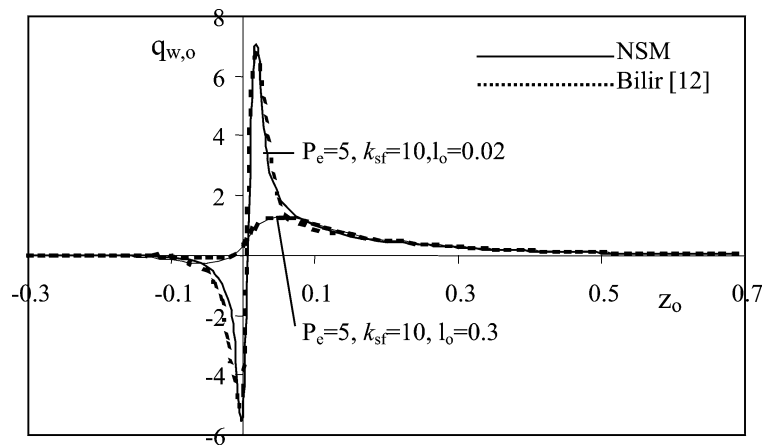
$$Nu = \frac{-2q_{w,o}}{(T_{w,o} - T_{b,o})} \quad (5c)$$

3. Numerical results

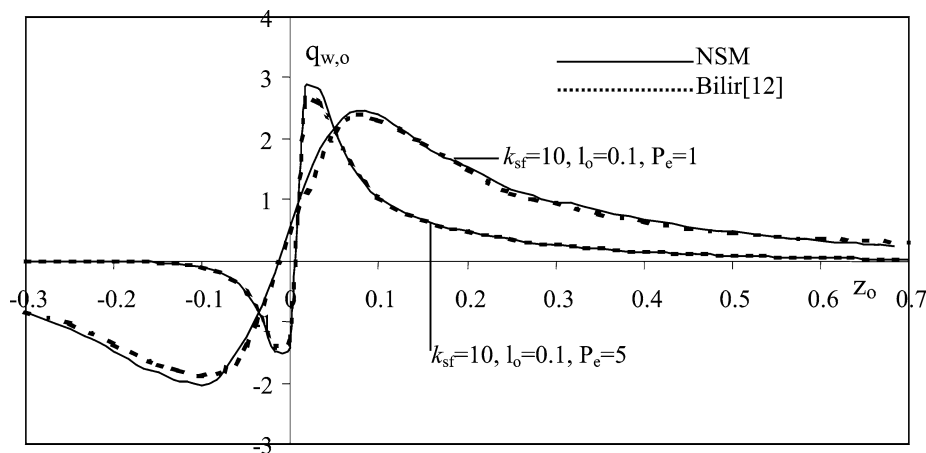
The steady-state results for the local interfacial heat flux, $q_{w,o}$, which gives more meaningful information than other parameters, are compared with those obtained by Bilir [12], using finite difference methods (see Fig. 2). The effects of the pipe thickness and Péclet number are shown separately in Figs. 2(a) and 2(b). An interpretation of the trend of $q_{w,o}$ in the curves may be found in the paper of Bilir [12]. In Fig. 3 values of the axial distribution of interfacial heat flux ($q_{w,o}$) for steady-state are given for different Péclet numbers and pipe thickness, with $k_{sf} = 1$. The figures show that at the downstream side of the pipe the curves rise to a maximum value and then decrease, due

Table 1

	Dimensionless boundary and initial conditions	
	Transient problem (with wall)	Graetz problem (without wall)
At $z_o = -\infty$	$T_{o,f} = T_{o,s} = 0$	$T_{o,f} = 0$ (3a)
At $z_o = +\infty$	$\partial T_{o,s} / \partial r_o = \partial T_{o,f} / \partial r_o = 0$ (3b)	$\partial T_{o,f} / \partial r_o = 4$ (3c)
At $r_o = 0$	$\partial T_{o,f} / \partial r_o = 0$	$\partial T_{o,f} / \partial r_o = 0$ (3d)
At $r_o = 1$	$T_{o,s} = T_{o,f}$ (3e)	—
	$k_{sf} \partial T_{o,s} / \partial r_o = \partial T_{o,f} / \partial r_o$ (3f)	
At $r_o = 1 + l_o$, $z_o < 0, t_o > 0$	$T_{o,s} = 0$ (3g)	$\partial T_{o,f} / \partial r_o = 0$ (3h)
At $r_o = 1 + l_o$, $z_o \geq 0, t_o > 0$	$T_{o,s} = 1$ (3i)	$\partial T_{o,f} / \partial r_o = 1$ (3j)
$\forall r_o, z_o, t_o = 0$	$T_{o,f} = T_{o,s} = 0$ (4)	—



(a)



(b)

Fig. 2. Comparison of the results. (a) Effect of thickness ratio for $Pe = 5$, $k_{sf} = 10$, $l_o = 0.02$ and $l_o = 0.3$. (b) Effect of Péclet's number for $l_o = 0.1$, $k_{sf} = 10$, $Pe = 1$ and $Pe = 5$.

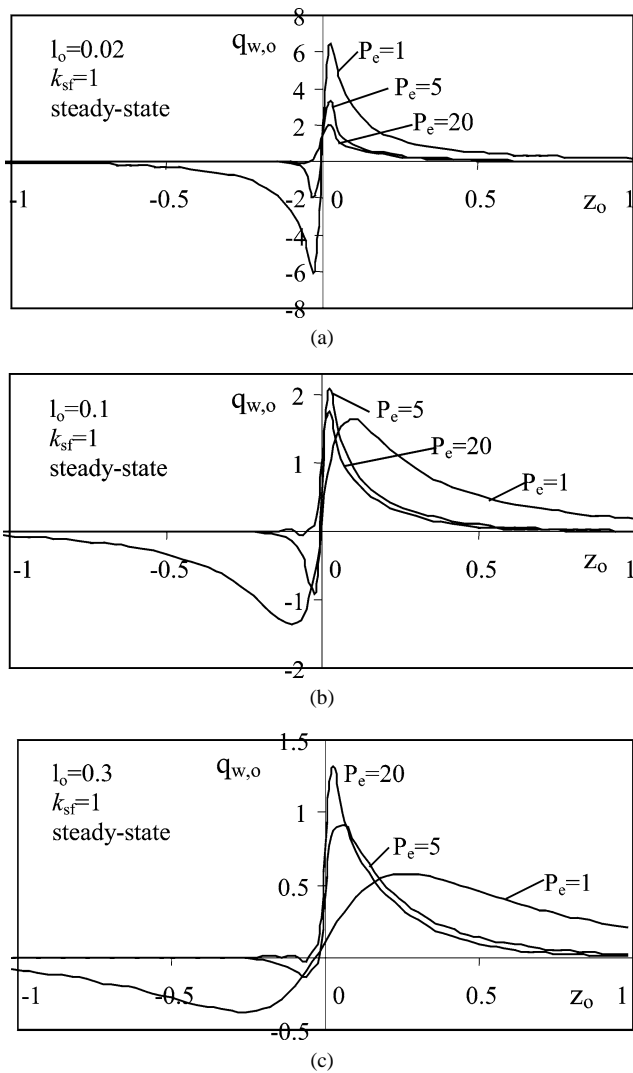


Fig. 3. Interfacial heat flux, $q_{w,o}$, at the steady-state for $k_{sf} = 1$. (a) Péclet's number = 1, 5 and 20, $l_o = 0.02$; (b) Péclet's number = 1, 5 and 20, $l_o = 0.1$; (c) Péclet's number = 1, 5 and 20, $l_o = 0.3$.

to the high temperature gradients at the beginning of the heating section. It can be seen that the maximum values are achieved when the pipe thickness decreases, because the thermal resistance of the pipe wall is smaller for thin walls and the heat supplied from the outer surface is easily transferred to the inner surface. After a certain axial distance, convection predominates over wall conduction, and heat flux values decrease. The effect of the Péclet number is as follows: when the pipe thickness is low ($l_o = 0.02$, Fig. 3(a)) on both the upstream and downstream side, the extent and the magnitude of the reverse (from fluid to wall) and direct (from wall to fluid) heat flux increase with a decreasing Péclet number; when the pipe thickness is high ($l_o = 0.3$, Fig. 3(c)) on the upstream side, the extent and the magnitude of the reverse heat flux, as before, increase with a decreasing Péclet number, while on the downstream side, although the extent of the direct heat flux also increases with decreasing Péclet number (since the convective effect

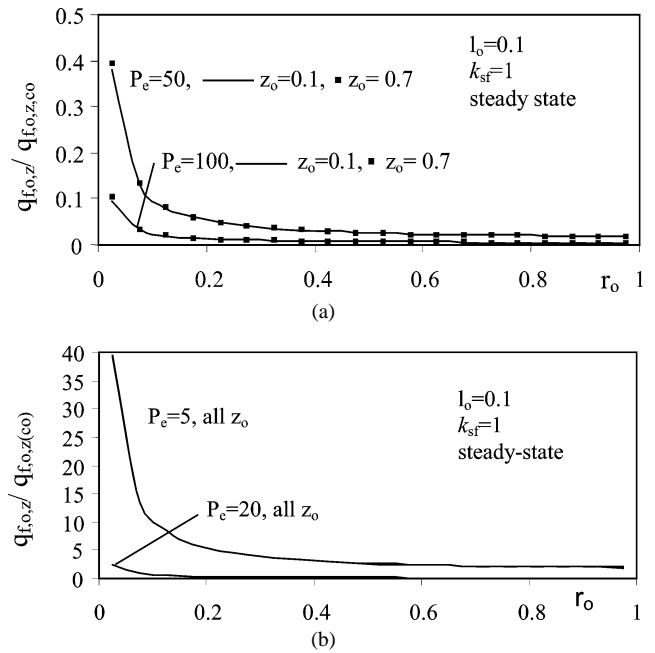


Fig. 4. Axial conduction-convection heat flux ratio: (a) $Pe = 100$ and 50 , (b) $Pe = 20$ and 5 .

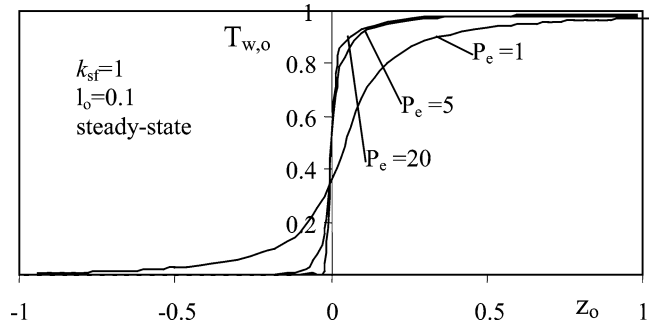


Fig. 5. Interfacial temperature, $T_{w,o}$, at the steady-state. Péclet's number = 1, 5 and 20, $k_{sf} = 1$ and $l_o = 0.1$.

is low and so the development length is greater), the magnitude (degree of peak) decreases with decreasing Péclet number.

The influence of the Péclet number on axial conduction is analysed in Figs. 4 and 5, with $l_o = 0.1$ and $k_{sf} = 1$. It can be seen that the ratio between fluid axial conduction and axial convection heat fluxes, $q_{f,o,z}/q_{f,o,z,co}$, diminishes as the radial position increases, and is negligible for $Pe > 100$ whatever the radial position. On the other hand, when the Péclet number increases the interfacial temperature is nearer the boundary condition, according to Fig. 5. Therefore the influence of the pipe thickness on the solution is also negligible for large Péclet numbers.

In the appendix (brief description of the Network Simulation Method), the resistors of the network model are obtained in the wall and fluid. The relation between the resistor axial conduction (Eq. (10d)) and the resistor axial convection

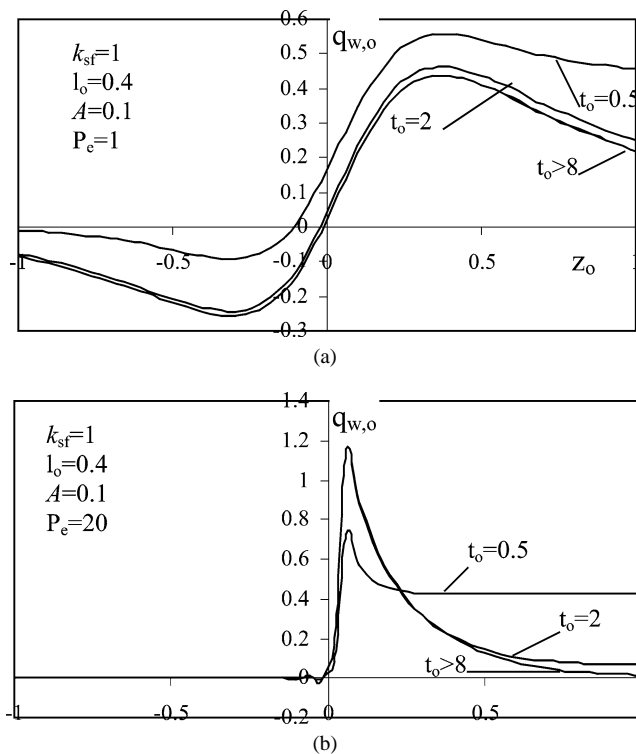


Fig. 6. Transient interfacial heat flux, $q_{w,o}$. $k_{sf} = 1$, $l_o = 0.4$ and $A = 0.1$. (a) $Pe = 1$, (b) $Pe = 20$.

(inverse of the control-voltage current-source G , Eq. (10e)), both in the fluid, is

$$R_{i \pm \Delta z/2, j} \cdot G_{i, j} = \frac{\Delta z(1 - r_{i, j}^2)}{2} Pe^2 = C_1(1 - r_{i, j}^2) Pe^2 \quad (6)$$

One should note that the ratio between the resistor axial conduction and resistor axial convection increases when Pe increases. It also increases in zones near the centre of the pipe, where $r_o(r/R)$ is small. These results are shown in Fig. 4. The effect of Pe in the transient is studied in Fig. 6 ($l_o = 0.4$, $A = 0.1$, $k_{sf} = 1$ and $Pe = 1$ and 20), where it can be seen that this parameter does not nearly influence the time required to reach the steady-state, because this time remains approximately constant, $t_{tran} \geq 8$.

Transient state is studied in Figs. 7 to 9 which represent interfacial temperature versus axial location. The influence of the parameters A and k_{sf} is clear from Fig. 7 for the dimensionless time $t_o = 1$, with $Pe = 5$ and $l_o = 0.3$. The magnitude achieved in steady-state is always independent of the value of the diffusivity ratio. For $A \geq 1$, the system is in steady-state and it takes longer to reach this state (upper curve) with smaller values of A and of k_{sf} . Anyway, due to the kind of boundary conditions (isothermal) involved in the problem under study, the steady-state is reached rapidly, which is not the case, for example, for the ambient convective boundary condition (Wei-Mon Yan [17]). In our work, the times to reach steady state for the cases analysed in Fig. 7 are:

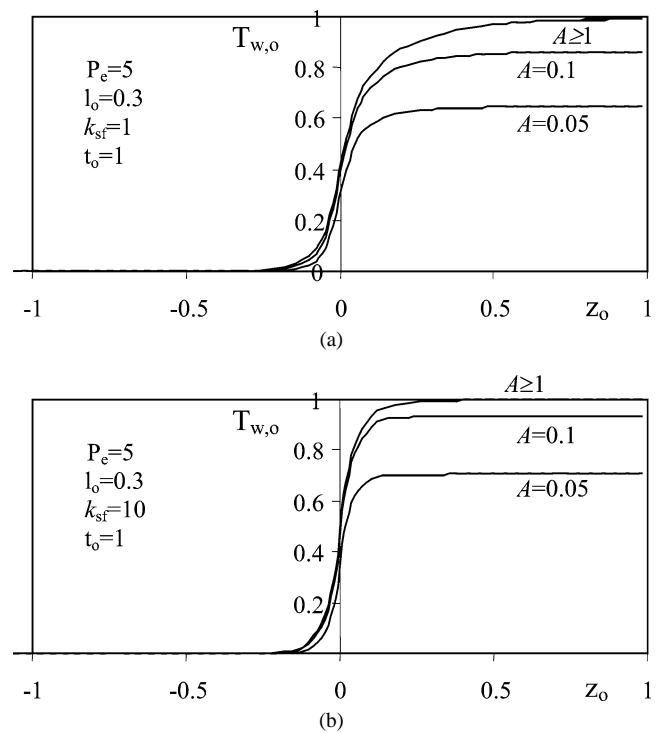


Fig. 7. Transient interfacial temperature, $T_{w,o}$. $Pe = 5$, $l_o = 0.3$ and $t_o = 1$. (a) Diffusivity ratio = 0.05 and 0.1, $k_{sf} = 1$. (b) Diffusivity ratio = 0.05 and 0.1, $k_{sf} = 10$.

case (a) $k_{sf} = 1$, for $A = 0.05$, $t_{o,tran} = 3.4$ and
for $A = 0.1$, $t_{o,tran} = 2.1$

case (b) $k_{sf} = 10$, for $A = 0.05$, $t_{o,tran} = 3.0$ and
for $A = 0.1$, $t_{o,tran} = 1.8$

On the other hand, in the wall, the transient is defined by means a condenser of value $C_{i, j} = k_{sf} \cdot r_{i, j} \cdot \Delta r_s / A$ (see Appendix A). When A increases, $C_{i, j}$ decreases, the energy storage capacity of the wall decreases and the time required to reach the steady-state also decreases.

The influence of the parameter k_{sf} on the interfacial temperature, $T_{w,o}$, is shown in Fig. 8 for the steady-state and for the dimensionless times $t_o = 0.5$ and 1 , with $Pe = 5$, $l_o = 0.3$ and $A = 0.05$. In this case the magnitude achieved in steady-state is dependent on the value of k_{sf} . Again, the time required to reach the steady-state is longer for smaller values of k_{sf} because of the great thermal capacity of the pipe. When $k_{sf} \geq 10$ the transient regimen remains approximately constant. It can also be seen that when k_{sf} increases, the effect of wall conduction on heat transfer decreases, for the same reasons as explained in Fig. 5.

The times to reach steady state for the case analysed in Fig. 7 are:

$$k_{sf} = 0.1, \quad t_{o,tran} = 4.2, \quad k_{sf} = 1.0, \quad t_{o,tran} = 3.5,$$

$$k_{sf} = 10, \quad t_{o,tran} = 2.9 \quad \text{and} \quad k_{sf} = 100, \quad t_{o,tran} = 2.8$$

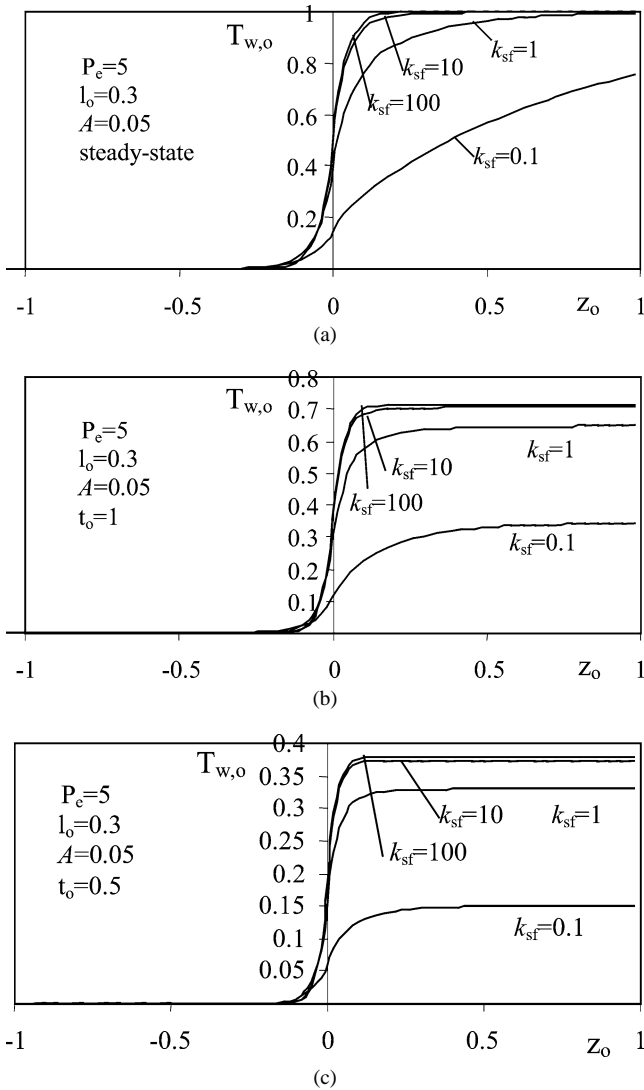


Fig. 8. Transient and steady-state response of the interfacial temperature, $T_{w,o}$. $Pe = 5$, $l_o = 0.3$ and $A = 0.05$. $k_{sf} = 0.1, 1, 10$ and 100 . (a) Steady-state, (b) $t_o = 1$, (c) $t_o = 0.5$.

The relation between the resistor fluid radial conduction (Eq. (10c)) and resistor wall radial convection (Eq. (10a)) can be expressed as

$$\frac{R_{i,j \pm \Delta r/2} |f}{R_{i,j \pm \Delta r/2} |s} = \frac{\Delta r_f}{\Delta r_s} k_{sf} = C_2 k_{sf} \quad (7a)$$

The same relation for axial conduction (Eq. (10d)) and resistor wall radial convection (Eq. (10b)) is

$$\frac{R_{i \pm \Delta z/2, j} |f}{R_{i \pm \Delta z/2, j} |s} = \frac{\Delta r_s}{\Delta r_f} k_{sf} = C_2^{-1} k_{sf} \quad (7b)$$

One should note that the relation between the resistor fluid conduction and resistor wall conduction (radial and axial) increases when k_{sf} increases and the effect of wall conduction on heat transfer decreases, because the heat in the wall is conducted more rapidly.

The influence of the thickness ratio l_o on the interfacial temperature, $T_{w,o}$, is shown in Fig. 9 for the steady-state

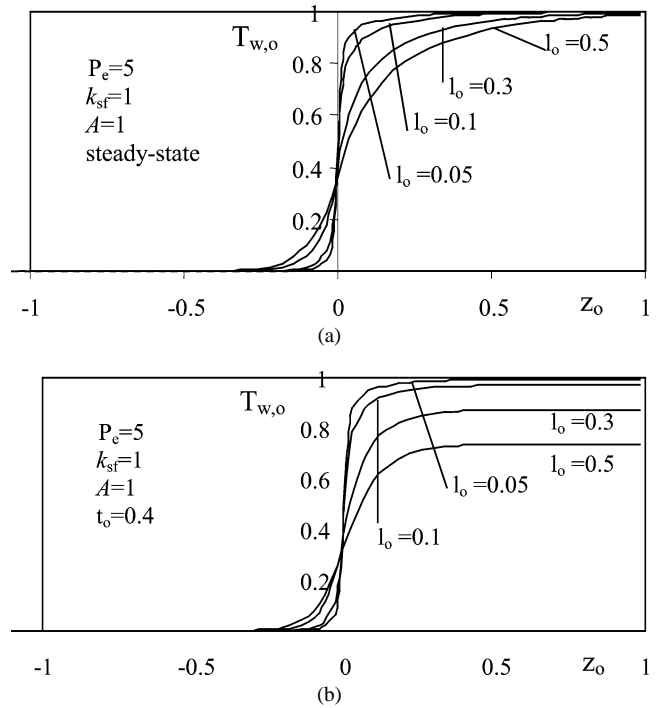


Fig. 9. Transient interfacial temperature, $T_{w,o}$. $Pe = 5$, $k_{sf} = 1$ and $A = 1$. $l_o = 0.05, 0.1, 0.3$ and 0.5 . (a) Steady-state, (b) $t_o = 0.4$.

Table 2
Comparison of local Nusselt numbers for uniform heat flux at the steady-state ($Pe = 5$)

Value of z_o	Value of Nu		
	Ref. [2]	Ref. [13] 20 × 80	Present method 20 × 100
0.010	7.09	7.20	7.18
0.020	6.39	6.45	6.44
0.050	5.50	5.45	5.46
0.100	4.82	4.85	4.87
0.200	4.47	4.51	4.53
0.300	4.40	4.42	4.43
∞	4.36	4.36	4.36

and for $t_o = 0.4$, $Pe = 5$, $k_{sf} = 1$ and $A = 1$. In this case, the time required to reach the steady-state increases with increasing l_o , because the energy storage capacity of the wall increases for larger thickness ratios. It is also evident that when l_o increases, the effect of wall conduction on heat transfer increases, because if this were not so, the boundary conditions of the heated wall would quickly reach the interfacial area.

The times taken to reach steady state for the case analysed in Fig. 9 are:

$$l_o = 0.05, \quad t_{o,tran} = 0.4, \quad l_o = 0.1, \quad t_{o,tran} = 0.5, \\ l_o = 0.3, \quad t_{o,tran} = 1.2 \quad \text{and} \quad l_o = 0.5, \quad t_{o,tran} = 1.6$$

Finally, the Nusselt numbers are given in Table 2 for different axial positions of the pipe for $Pe = 5$ and for the case of uniform heat flow with the wall in steady-state. The results are very close in all the cases.

4. Concluding remarks

The conjugated heat transfer problem for laminar flows in pipes (including bi-dimensional wall and axial conduction in the fluid) is studied both for the transient and steady-states. This study uses the network simulation method, which is specially useful when hard non-linearities are present in the equations of the process. This numerical tool requires none of mathematical manipulations inherent in the resolution of the finite-difference equations. Instead, the software selected to solve the circuits does this work. On the other hand, the method permits direct visualisation and evaluation of the main variables of the transport phenomena (heat flux and temperature) which are equivalent to the electric variables, current and potential. PSPICE [20], the software selected in this work, has a vast library of non-linear electric devices which are suitable for an easy implementation of the non-linear processes involved in the problem. In this work, the computation time was a few seconds. Furthermore, it is very easy and fast to make changes in the boundary and initial conditions of the problem. To obtain the stationary response, the condenser of the network merely has to be omitted.

The results obtained have been compared with the results of other authors and are very close.

The main results of the investigation may be briefly summarized as follows:

- It is important consider wall conduction because it plays a significant role in a transient conjugated heat transfer problem.
- For larger values of the Péclet number, the fluid axial conduction will be negligible, indicating that the results mainly depend on the wall characteristics rather than on flow conditions.
- The time required to reach the steady-state is longer for smaller values of k_{sf} and A or larger values of l_o , and is independent of the Péclet number. This time varies very little with variations in these parameters.
- The effect of wall conduction on heat transfer increases as the Péclet number and k_{sf} decrease and l_o increases. In the contrary case, it is possible to eliminate the wall to study the system.

Appendix A. A brief description of the Network Simulation Method

As regards this numerical method, which is based on the existing analogy between electric circuit theory and heat conduction theory, it should be emphasised that it has nothing to do with the classical thermo-electrical analogy. NSM is widely used in many text books and its aim is not other than an alternative symbolic representation of the simple heat transfer problems [22]. The main feature of the physically-inspired NSM is the use of discrete intervals for the spatial variable (the time variable being a

continuous function), a development that is also adopted by the mathematically oriented Method of Lines [23].

A new set of ordinary differential equations is obtained by spatial discretization of the mathematical model defined by a set of equations that includes: (i) heat conduction equation, (ii) boundary conditions, (iii) initial condition and (iv) special conditions, while t is maintained as a continuous independent variable. With this end in view, the whole 2-D region is divided into a number of volume elements or cells which are not necessarily similar. A network model for an elementary cell is designed from this set of equations, associating different kinds of electrical ports to each one of the terms that integrate the differential equations: resistors, capacitors, and non-linear electrical devices. The model for the whole medium is obtained by connecting N elemental networks in series. Boundary conditions are implemented by additional electrical devices connected to the boundaries. By selecting $N \geq 30$ for axial and radial directions, errors are reduced to values below 0.5% in 2-D problems [24]. In the axial direction, the regions near $z = 0$ have been discretized with fine grids to increase accuracy, using coarse grids in other regions. The axial distance ensures that the boundary conditions in $z = \pm\infty$.

As regards the problem studied here, the geometry of the cells is a circular crown whose surface section has a dimension of Δr_f , Δr_s and Δz . The numbers of cells in the radial and axial directions are $N_{r,f}$, $N_{r,s}$ and N_z . The following expressions are applied:

$$\Delta r_f = r_o / N_{r,f}, \quad \Delta r_s = l_o / N_{r,s} \quad \text{and} \quad \Delta z = 2 / N_z.$$

Discretization of Eqs. (1) and (4) for the pipe and (2) for the fluid yield the following ordinary differential equations in dimensionless form:

$$\begin{aligned} & [T_{i,j-\Delta r/2} - T_{i,j}] / (r_{i,j} \Delta r_s) [2k_{sf} r_{i,j-\Delta r/2} / \Delta r_s] \\ & - [T_{i,j} - T_{i,j+\Delta r/2}] / (r_{i,j} \Delta r_s) [2k_{sf} r_{i,j+\Delta r/2} / \Delta r_s] \\ & + [T_{i-\Delta z/2,j} - T_{i,j}] / (Pe^2 \Delta z) [2k_{sf} / \Delta z] \\ & - [T_{i,j} - T_{i+\Delta z/2,j}] / (Pe^2 \Delta z) [2k_{sf} / \Delta z] \\ & = k_{sf} / A \, dT_i / dt \end{aligned} \quad (8)$$

$$\begin{aligned} & [T_{i,j-\Delta r/2} - T_{i,j}] / (r_{i,j} \Delta r_f) [2r_{i,j-\Delta r/2} / \Delta r_f] \\ & - [T_{i,j} - T_{i,j+\Delta r/2}] / (r_{i,j} \Delta r_f) [2r_{i,j+\Delta r/2} / \Delta r_f] \\ & + [T_{i-\Delta z/2,j} - T_{i,j}] / (Pe^2 \Delta z) [2 / \Delta z] \\ & - [T_{i,j} - T_{i+\Delta z/2,j}] / (Pe^2 \Delta z) [2 / \Delta z] \\ & = (1 - r_{i,j}^2) [T_{i+\Delta z/2,j} - T_{i-\Delta z/2,j}] / \Delta z + dT_i / dt \end{aligned} \quad (9)$$

where $T_{i,j}$, $T_{i,j+\Delta r/2}$, $T_{i,j-\Delta r/2}$, $T_{i+\Delta z/2,j}$, $T_{i-\Delta z/2,j}$, are the temperatures in the centre and ends of the cell, respectively (Fig. 10(a); suffix o , which refers to dimensionless form, has been omitted for simplicity). The convection heat flux on the surface of each control volume is taken by a special electrical device named “control-voltage current-source”, G , which shows a non-linear behaviour. The current of these generators may be defined as an arbitrary function

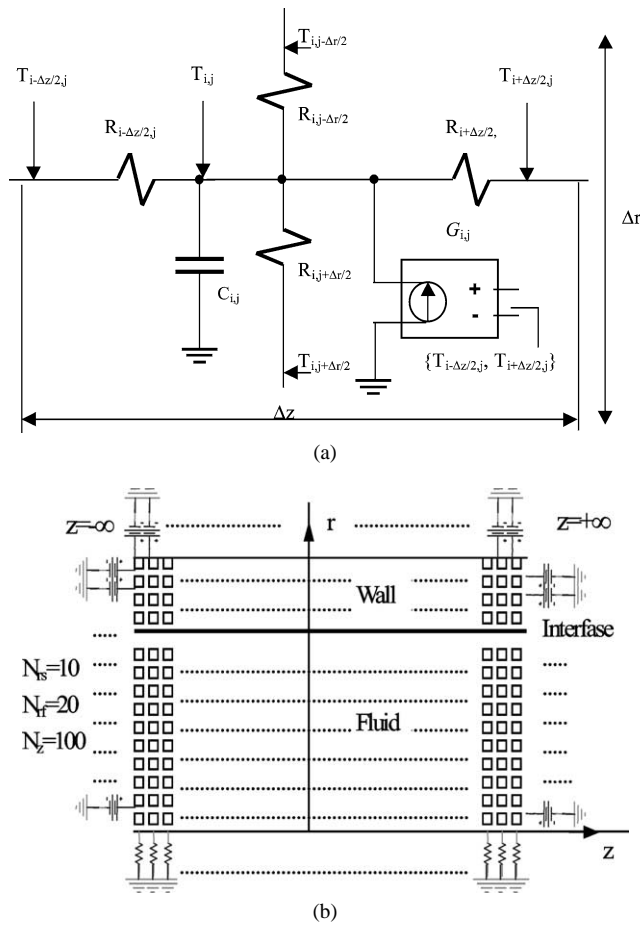


Fig. 10. (a) Network model for pipe and fluid. (b) Network discretization and boundary conditions.

of one or more voltages in the cell. The network model for a fluid cell is shown in Fig. 10(a); the network model for a pipe cell is the same but without the resistor $R_{i,j}$. Each cell is electrically connected to contiguous cells to make up the whole model of the medium (Fig. 10(b)).

For the wall, the network model is composed of four resistors,

$$R_{i,j\pm\Delta r/2} = \frac{\Delta r_s}{2k_{sf}r_{i,j\pm\Delta r/2}} \quad (10a)$$

and

$$R_{i\pm\Delta z/2,j} = \frac{\Delta z^2 Pe^2}{2k_{sf}r_{i,j} \Delta r_s} \quad (10b)$$

and a condenser of value $C_{i,j} = k_{sf} \cdot r_{i,j} \cdot \Delta r_s / A$ (Fig. 10a).

For the fluid network model, the values for the resistors are

$$R_{i,j\pm\Delta r/2} = \frac{\Delta r_f}{2r_{i,j\pm\Delta r/2}} \quad (10c)$$

$$R_{i\pm\Delta z/2,j} = \frac{\Delta z^2 Pe^2}{2r_{i,j} \Delta r_f} \quad (10d)$$

The value of the capacitor is $C_{i,j} = r_{i,j} \cdot \Delta r_f$, and the voltage-control current-source

$$G_{i,j} = \frac{(1 - r_{i,j}^2)r_{i,j} \Delta r_f}{\Delta z} \quad (10e)$$

Fig. 9(b) is a scheme of the devices that implement the boundary conditions. The values of the parameters used in this problem are: $N_{r,f} = 20$, $N_{r,s} = 10$, $N_z = 100$, $\Delta r_f = 1/20$, $\Delta r_s = l_o/10$, $\Delta z = 2/100$.

It should be mentioned that heat conservation is satisfied since Kirchhoff conservation law for the electric currents is inherent in the networks. In this way, no additional conditions are needed to ensure this condition. The uniqueness of the temperature variable is also satisfied due to Kirchhoff voltage law. Once we have obtained the general network model, its simulation provides the temporal evolution and stationary values of the heat flux and temperature variables in the cell. Very few language program rules are necessary to make the program files run on PSPICE software, and those that are necessary are straightforward. Once the network model for a cell is programmed, PSPICE recognises it as a sub-circuit that may be implemented as many times as is required, which simplifies the program. The interactive design warns the programmer of possible errors and depicts the correct way of acting. It is simply necessary the spatial discretization of the equations (with no subsequent mathematical manipulation of these equations by the user); therefore, the time interval to obtain the numerical solution is imposed and adjusted continuously by Pspice automatically to reach a convergent solution in each iteration.

References

- [1] L. Graetz, Über die Wärmeleitfähigkeit von Flüssigkeiten, Part 1, Ann. Phys. Chem. 18 (1983) 79–94;
L. Graetz, Über die Wärmeleitfähigkeit von Flüssigkeiten, Part 2, Ann. Phys. Chem. 25 (1985) 337–357.
- [2] L. Graetz, M. Sakakibara, A. Tanimoto, Steady heat transfer to laminar flow in a circular tube with conducting in wall, Heat Transfer Jap. Res. 3 (1974) 37–46.
- [3] S. Mori, M. Shinke, M. Sakakibara, A. Tanimoto, Steady heat transfer to laminar flow between parallel plates with conducting in wall, Heat Transfer Jap. Res. 5 (1976) 17–25.
- [4] M.L. Michelsen, J. Willadsen, The Graetz problem with axial heat conduction, Int. J. Heat Mass Transfer 17 (1974) 1391–1402.
- [5] G. Pagliriani, Effect of axial conduction in the wall and the fluid on conjugate heat transfer in thick-walled circular tubes, Int. Comm. Heat Mass Transfer 55 (1988) 5881–5891.
- [6] B. Vick, M.N. Özisik, An exact analysis of low Péclet number heat transfer in laminar flow with axial conduction, Lett. Heat Transfer 8 (1981) 1–10.
- [7] N.J. Wijesundera, Laminar forced convection in circular and flat ducts with wall axial conduction and external convection, Int. J. Heat Mass Transfer 29 (1986) 797–807.
- [8] R.O.C. Guedes, R.M. Cotta, N.C.L. Brum, Heat transfer in laminar flow with wall axial conduction and external convection, J. Thermophys. 5 (1990) 4.

- [9] H.Y. Zhang, M.A. Ebadian, A. Campo, Effects of heat generation and axial heat conduction in laminar flow inside a circular pipe with a step change in wall temperature, *Trans. ASME J. Heat Transfer* 102 (1980) 58–63.
- [10] E.K. Zariffah, H.M. Soliman, A.C. Trupp, The combined effect of wall and fluid axial conduction on laminar heat transfer in circular tubes, *Heat Transfer* 4 (1982) 131–135.
- [11] A. Campo, R. Rangel, Lumped system analyses for the simultaneous wall and fluid axial conduction in laminar pipe flow heat transfer, *Physicochem. Hydrodyn.* 4 (1983) 163–173.
- [12] S. Bilir, Laminar flow heat transfer in pipes including two-dimensional wall and fluid axial conduction, *Int. J. Heat Mass Transfer* 38 (9) (1995) 1619–1625.
- [13] S. Bilir, Numerical solution of Graetz problem with axial conduction, *Numer. Heat Transfer, Part A* 21 (1992) 493–500.
- [14] R.M. Cotta, M.D. Mikhailov, M.N. Özisik, Transient conjugated forced convection in ducts with periodically varying inlet temperature, *Int. J. Heat Mass Transfer* 30 (10) (1986) 2073–2082.
- [15] W. Li, K. Sadik, Unsteady thermal entrance heat transfer in laminar with a periodic variation inlet temperature, *Int. J. Heat Mass Transfer* 34 (10) (1991) 2581–2592.
- [16] S. Olek, E. Elias, E. Wacholder, S. Kaizerman, Unsteady conjugated heat transfer in laminar pipe flow, *Int. J. Heat Mass Transfer* 34 (6) (1991) 1443–1450.
- [17] Wei-Mon Yan, Transient conjugated heat transfer in channel flows with convection from the ambient, *Int. J. Heat Mass Transfer* 36 (5) (1993) 1295–1301.
- [18] F. Alhama, J.F. López-Sánchez, C.F. González-Fernández, Heat conduction through a multilayered wall with variable boundary conditions, *Energy* 22 (1997) 797–803.
- [19] C.F. González-Fernández, F. Alhama, J.F. López Sánchez, Application of the network method to heat conduction processes with polynomial and potential-exponentially varying thermal properties, *Numer. Heat Transfer, Part A, Appl.* 33 (1998) 549–559.
- [20] J. Horno (Ed.), *Network Simulation Method*, Research Signpost, Trivandrum, Kerala, India, 2002.
- [21] PSPICE, v. 6.0: Microsim Corporation, 20 Fairbanks, Irvine, California 92718, 1994.
- [22] A.F. Mills, *Heat and Mass Transfer*, Richard D. Irwin, 1995.
- [23] O.A. Liskovets, The method of lines (review), *Differential Equations* 1 (1965) 1308–1323.
- [24] F. Alhama, *Transient thermal responses in nonlinear heat conduction processes*, Ph.D. Thesis, University of Murcia, Spain, 1999.